Microhardness anisotropy on the (010) cleavage plane of single crystals of Bi_2S_3 and Sb_2S_3

HONG LI, M. JENSEN, R. C. BRADT
The Mackay School of Mines, University of Nevada, Reno, Nevada 89557-0047, USA

Knoop microhardnesses were measured on the (010) cleavage planes of Bi_2S_3 and Sb_2S_3 single crystals for orientations from the [001] to the [100]. The [001] hardnesses were nearly twice the level of the [100] values, about 150–75 kg mm^{-2}. The experimental microhardness profile was consistent with the calculated effective resolved shear stress (ERSS) diagram for the (010) [001] primary slip system. The magnitude of the hardness appears to be related to the crystal structure, particularly the metal–sulphur chains parallel to the [001], the crystal growth direction.

1. Introduction

Bismuthinite (Bi_2S_3) and stibnite (Sb_2S_3) are two semiconducting sulphides found in nature, which, in addition to guanajuatite, (Bi_2Se_3) comprise the stibnite group. Most research studies of these materials have focused on their unique electrical or optical properties and the related applications [1–7]. However, the utilization of these sulphides often focuses on their mechanical properties as a major point of concern. With the exception of several hardness values, relatively little has been published regarding their mechanical properties. On the Moh's scale, the hardness has been reported to be 3–3.75 for Bi_2S_3 and 2.75–3.5 for Sb_2S_3 [8]. Vickers microhardnesses have also been reported for both of these sulphides, ranging from 67–216 kg mm^{-2} for Bi_2S_3 and from 42–153 kg mm^{-2} for Sb_2S_3 [9, 10].

In their classical microhardness paper, Young and Millman [11] have reported Vickers microhardness values for Bi_2S_3 and Sb_2S_3 single crystals on the (001), (010) and (100) planes. Their results indicate that a significant microhardness difference exists between these three crystallographic planes, suggesting that the hardness of these crystals is highly anisotropic. However, there was no information on the specific indenter orientations for which the Vickers microhardnesses were measured on those planes. Nevertheless, the Young and Millman study does suggest that Bi_2S_3 is harder than Sb_2S_3 on the (010) cleavage planes.

Arivuoli. *et al.* [12] have also reported Vickers microhardnesses, but for synthetic Bi_2S_3 and Sb_2S_3 single crystals, suggesting that Sb_2S_3 is about five times as hard as Bi_2S_3, approximately 100 kg mm^{-2} versus only 20 kg mm^{-2}. This contradicts the previous reports which, when comparing the microhardnesses, suggest that Bi_2S_3 is harder than Sb_2S_3. Vengatesan *et al.* [13] have also published a microhardness value of 131 kg mm^{-2} for single crystal stibnite, nearly 50%

higher than the hardness level reported by Arivuoli *et al.* [12]. As the above studies contain several contradictions and none report the complete crystallography of the hardness measurements (crystal plane plus indenter orientation), these interesting materials merit additional hardness studies. This paper reports a detailed study of the microhardness anisotropy on the (010) cleavage planes of these two sulphide crystals.

2. Experimental procedure

Natural single crystals of Bi_2S_3 and Sb_2S_3 were obtained for this study from the Victoria Mine, Elko County, Nevada, USA and the White Caps Mine, Nye County, Nevada, USA, respectively. They were a shiny metallic grey in appearance and in the form of a viburnum cluster of rod-like shapes, varying in size to about a centimeter in diameter. These crystals are both orthorhombic with the space group P b n m [14] and have an [001] growth direction. Chemical analyses of these crystals were made utilizing the energy dispersive spectroscopy (EDS) technique on a Jeol JSM–840A scanning electron microscope. Fig. 1 depicts the two analysis traces, revealing that no major impurities are present in either of the two sulphide crystals.

For the microhardness measurements of this study, several of the larger rod-shaped crystals were extracted from the viburnum clusters. Because of their distinct (010) cleavage, test specimens of that plane were readily obtained for measurements of the Knoop microhardness anisotropy. Once suitable (010) plane specimens were obtained, they were mounted and polished first with a 15 μm Al_2O_3 slurry then with 5, 3, 1, and finally 0.25 μm diamond paste to yield a mirror-like surface finish that was acceptable for subsequent Knoop microhardness measurements.
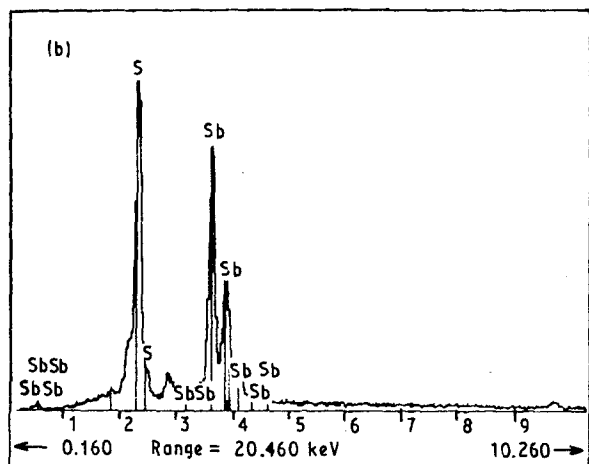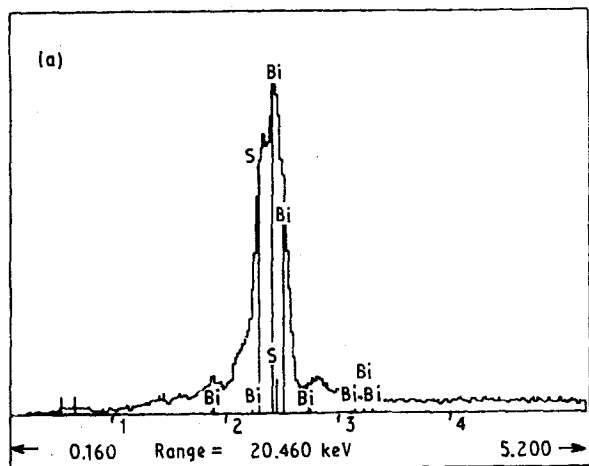
Figure 1 EDS analyses of the single crystals of: (a) Bi_2S_3 and (b) Sb_2S_3 on the (0 1 0) cleavage planes.

Azimuthal angle from [001] to [100] on the (010)
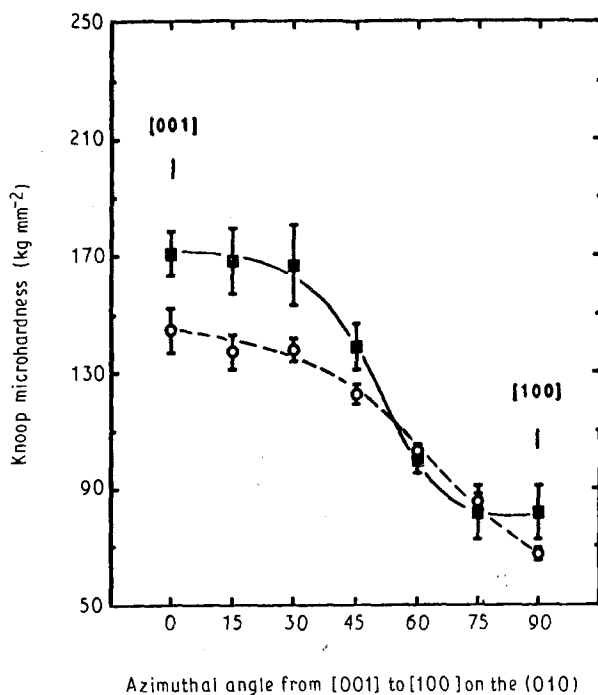
Figure 2 Knoop microhardness on the (0 1 0) cleavage planes for single crystals of: (■) Bi_2S_3 and (○) Sb_2S_3, for a test load of 25 g.

Microhardness measurements were completed for orientations of the long diagonal of the Knoop indenter parallel to the [0 0 1] to an orientation parallel to the [1 0 0] at 15° intervals. Indentations were made at room temperature at a test load of 25 g and an identation rate of 0.017 mm s^{-1} for a dwell time of 15 s. In spite of the excellent polish of the specimen surfaces, severe cracks, both cleavage and non-cleavage types, emanated from the identations at all attempted test loads above 25 g, thus not allowing for reliable hardness measurements at loads above the 25 g level. Immediately after each indentation, the length of the long diagonal of the Knoop impression was measured. Microhardnesses were calculated from the long diagonal length by

$$KHN = 14.229 \frac{P}{d^2} \quad (kg\,mm^{-2}) \qquad (1)$$

where P is the indentation test load (in kilograms) and d is the long diagonal of the Knoop impression (in millimetres). The Knoop microhardness values are reported as the averages for 25 individual indentations at each indentation orientation with their 95% confidence intervals calculated by the t-distribution.

3. Results and discussion

Fig. 2 illustrates the Knoop microhardness profiles for Bi_2S_3 and Sb_2S_3 on their (0 1 0) cleavage planes. It is evident that the over-all shapes of the Knoop microhardness anisotropy profiles for these two crystals are very similar, exhibiting only minor differences. For the (0 1 0) cleavage planes of these orthorhombic sulphide crystals, the maximum microhardness is observed when the long diagonal of the Knoop indenter is parallel to the [0 0 1], the rod-like crystal growth direction. The minimum microhardness occurs when the indenter long diagonal is parallel to the [1 0 0] direction. It is evident that the Knoop microhardnesses of these two crystals are highly anisotropic on the (0 1 0), varying by a factor of about two; from 81.6–170.6 kg mm^{-2} for the Bi_2S_3 and from 67.4–137.1 kg mm^{-2} for the Sb_2S_3. The microhardness anisotropy for these two sulphides, defined as $(KHN_{max} - KHN_{min})/KHN_{min}$, exceeds 100%, as it is 109% for the Bi_2S_3 and 103% for the Sb_2S_3. The microhardnesses of these two crystals are at about the 2.5–3 level on the Mohs' scale and compare favourably to the previously reported values [8].

As evident in Fig. 2, the microhardness profiles of these two orthorhombic sulphides are very similar. However, Bi_2S_3 is harder than Sb_2S_3 for the [0 0 1] and most other orientations on the (0 1 0) cleavage plane, but it is nearly equal in microhardness to Sb_2S_3 as the indenter orientation approaches the [1 0 0]. Except for the observations of Arivuoli *et al.* [12], other reports also suggest that Bi_2S_3 is harder than Sb_2S_3. Unfortunately, in the Arivuoli *et al.* paper, the crystallographic orientations, including the crystal planes and the indenter orientations during measurement, were not specified. For that reason, it is not possible to further address this major difference, for the extreme microhardness anisotropy that exists on the (0 1 0) cleavage plane suggests

that these hardness differences could easily be the result of hardness measurements on different crystal planes as well as for different crystallographic orientations on the same plane.

The shapes of microhardness anisotropy profiles can frequently be explained on the basis of the ERSS on the primary slip system during indentation. This concept has been advanced by Brookes et al. [15] and has been satisfactorily utilized to explain the Knoop microhardness anisotropy of numerous of single crystals. However, any applications of the ERSS concept to orthorhombic crystal structures have not been reported. It is constructive to apply that concept to these two sulphide crystals. Although there is a paucity of studies of the slip systems and dislocation processes for these crystals, Palache et al. [16] do cite the primary slip systems for both crystals as the $(0\,1\,0)$ $[0\,0\,1]$. It has been related to the crystal structure by Scavnicar [17] and Bayliss and Nowacki [18]. That reported primary slip system can be utilized in the analysis of the Knoop microhardness anisotropy by applying the ERSS concept.

Fig. 3 illustrates the calculated ERSS diagram for Knoop indentation on the $(0\,1\,0)$ cleavage plane for the $(0\,1\,0)$ $[0\,0\,1]$ primary slip system. The conditions of this calculation are based on: (a) the Knoop indenter being applied to the $(0\,1\,0)$ cleavage plane for long diagonal orientations from the $[0\,0\,1]$ to the $[1\,0\,0]$ and (b) of the $(0\,1\,0)$ $[0\,0\,1]$ primary slip system. Consideration of the unit cell dimensional differences between these two sulphide crystals was initially taken into account for the individual ERSS diagram calculations. However, the differences in the lattice parameters of the two crystals are too small to yield any distinguishable differences in the calculated ERSS diagrams, hence Fig. 3 represents the shape of the characteristic ERSS diagram for both

Azimuthal angle from [001] to [100] on the (010)
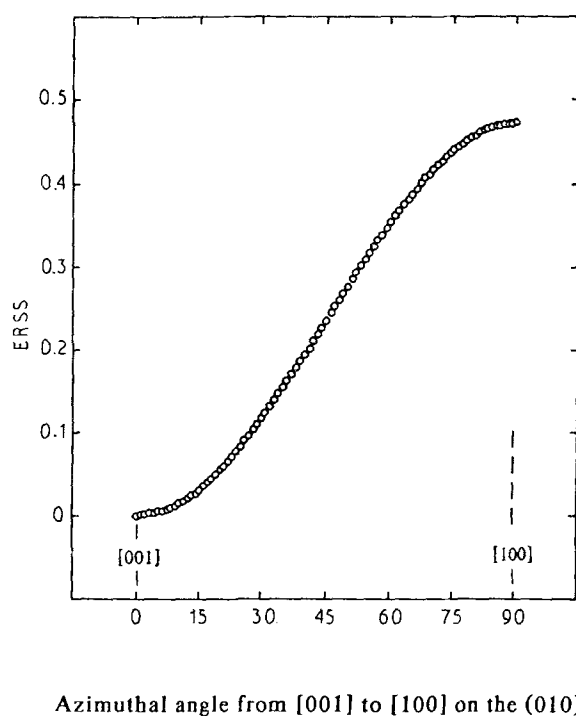
Figure 3 Effective resolved shear stress for Bi_2S_3 and Sb_2S_3 single crystals with respect to the $(0\,1\,0)$ $[0\,0\,1]$ primary slip system and Knoop indentation on the $(0\,1\,0)$ cleavage plane.

of these two sulphides. By comparing the calculated ERSS diagram in Fig. 3 with the experimentally measured microhardness anisotropy profile in Fig. 2, it is evident that the calculated ERSS diagram is inversely related to the experimental microhardness anisotropy profile, as expected. Based on this agreement between the experimental microhardness anisotropy profiles and the calculated ERSS diagram, the microhardness anisotropy from the $[0\,0\,1]$ to the $[1\,0\,0]$ on the $(0\,1\,0)$ of these two orthorhombic sulphide crystals may be directly associated with plastic deformation on the $(0\,1\,0)$ $[0\,0\,1]$ primary slip system.

In addition to the aforementioned effects of the $(0\,1\,0)$ $[0\,0\,1]$ primary slip system on the microhardness anisotropy, the structure of these sulphides appears to be equally important relative to the microhardnesses reported in Fig. 2. The crystal structures of Bi_2S_3 and Sb_2S_3 were first reported by Hofmann [14] and later refined by Scavnicar [17] and by Bayliss and Nowacki [18]. Their studies indicate that these two sulphides consist of double zigzag metal–sulphur chains of Bi(Sb) and S trigonal pyramids oriented parallel to the $[0\,0\,1]$, the natural growth direction of these rod-shaped crystals. The Bi–S(Sb–S) bonding perpendicular to these $[0\,0\,1]$ chains is much weaker. The weakest bonding is in the $[0\,1\,0]$, which explains the perfect $(0\,1\,0)$ cleavage for these sulphides [14, 17, 18]. On the basis of the structure and the bonding characteristics, it is not unexpected that the microhardness on the $(0\,1\,0)$ cleavage plane should be much higher in the $[0\,0\,1]$ than in the $[1\,0\,0]$. Indeed, the experimental microhardnesses reflect the characteristics of the oriented chain structure and metal–sulphur bonding in these two sulphides.

Applying similar structural and bonding arguments, it is possible to explain why the microhardness of Bi_2S_3 is greater than that of Sb_2S_3. Although both crystals have the same crystal structure, the bonding of Bi_2S_3 is stronger than that of Sb_2S_3, as revealed by their melting temperatures, which are generally indicative of bond strengths. For these two sulphides, Bi_2S_3 has a significantly higher melting temperature (760 °C) than Sb_2S_3 (556 °C) [19].

The difference of the microhardness between these two crystals is significantly narrowed when the indenter orientation is parallel to the $[1\,0\,0]$. This is probably related to the weak bonding in that orientation, as both the $[1\,0\,0]$- and $[0\,1\,0]$- bonding in these crystals are significantly weaker than the $[0\,0\,1]$. For indenter orientations near to the $[0\,0\,1]$, the hardness is dominated by the chain structure, while for the $[1\,0\,0]$ indenter orientation, the microhardness is dominated by the very weak bonding between the metal–sulphur chains. This suggests that these sulphides may be similar in microhardness in the $[1\,0\,0]$, and that any hardness differences may be expected to be amplified for the $[0\,0\,1]$ indenter orientation, exactly as observed experimentally. The microhardness differences between these two sulphides is related to their structure and bonding.

4. Summary and conclusions
The Knoop microhardness profiles of single crystals of Bi_2S_3 and Sb_2S_3 were experimentally determined for

the (0 1 0) cleavage planes. The bismuthinite appears to be slightly harder than the stibnite for most indenter orientations. The microhardnesses of these orthorhombic crystals are highly anisotropic, as the hardness for the [0 0 1] indenter orientations are nearly twice as hard as the [1 0 0] orientations on the (0 1 0) plane. The microhardness anisotropy profile is inversely related to the calculated effective resolved shear stress diagram for the (0 1 0) [0 0 1] primary slip system, which satisfactorily explains the shapes of the microhardness anisotropy profiles. The differences in the microhardnesses of these two sulphides appears to be related to the structure and bond strengths, particularly the metal–sulphur chain structure parallel to the [0 0 1], from which it may be concluded that both the microhardness anisotropy and the hardness levels are strongly interrelated.

References

1. W. TOKWDA, T. KATOH and A. YASUMORI, *J. Appl. Phys.* **45** (1974) 5098.
2. B. GHOSH and G. P. KOTHIYAL, *Proc. Cryst. Growth Charact.* **6** (1983) 393.
3. B. B. NAYAK and H. N. ACHARYA, *Thin Solid Films* **122** (1984) 93.
4. T. FUJITA, K. KURITA, K. TAKIYAMA and T. ODA, *J. Phys. Soc. Japn.* **56** (1987) 3734.
5. H. W. SUN, B. TANGUY, J. M. REAU, J. J. VIDEAU and T. PORTIER, *Mater. Res. Bull.* **22** (1987) 923.
6. A. CANTARERO, J. P. MARTINEZ, A. SEGURA and A. CHEVY, *Phys. Status Solidi A* **101** (1987) 603.
7. L. TICHY, H. TICHA, L. BENES and J. MALEK, *J. Non-Cryst. Solids* **116** (1990) 206.
8. A. S. POVARENNYKH, in "Crystal Chemical Classification of Minerals", Vol. 1 (Plenum Press, New York, 1972) p. 246.
9. D. J. VAUGAN and J. R. CRAIG, in "Mineral Chemistry of Metal Sulfides" (Cambridge University Press, London, 1978) pp. 381 and 401.
10. J. R. CRAIG and D. J. VAUGAN, in "Ore Microscopy and Ore Petrography" (John Wiley, New York, 1981) pp. 325 and 367.
11. B. B. YOUNG and A. P. MILLMAN, *Trans. Inst. Min. Metall.* **73** (1963–64) 437.
12. D. ARIVUOLI, F. D. GNANAM and P. RAMASAMY, *J. Mater. Sci. Lett.* **7** (1988) 711.
13. B. VENGATESAN, N. KANNIAH and P. RAMASAMY, *Mater. Sci. Eng.* **A104** (1988) 245.
14. W. HOFMANN, *Zeit. f. Krist.* **86** (1933) 225.
15. C. A. BROOKES, J. B. O'NEILL and B. A. W. REDFERN, *Proc. R. Soc. London* **A322** (1971) 73.
16. The System of Mineralogy, 7th Edn, edited by C. Palache, H. Berman and C. Frondel, Vol. 1 (John Wiley, New York, 1944) p. 270.
17. S. SCAVNICAR, *Zeit. f. Krist.* **114** (1960) 85.
18. P. BAYLISS and W. NOWACKI, *ibid.* **135** (1972) 308.
19. P. B. BARTON and B. J. SKINNER, in "Geochemistry of Hydrothermal Ore Deposits", edited by H. L. Barnes (Holt Rinehart & Winston, New York, 1967) p. 236.